COMPUTER SIMULATIONS OF HIGH-ENERGY HEAVY ION COLLISIONS

By

Gerd Kortemeyer

A DISSERTATION

Submitted to
Michigan State University
in partial fulfillment of the requirements
for the degree of

DOCTOR OF PHILOSOPHY

Department of Physics and Astronomy

1997

ABSTRACT

COMPUTER SIMULATIONS OF HIGH-ENERGY HEAVY ION COLLISIONS

By

Gerd Kortemeyer

One of the still most challenging questions in nuclear physics is that of the equation of state (EOS) of nuclear matter – how does nuclear matter change its properties under different temperatures and pressures? Is there a phase transition to quark gluon plasma? Heavy-ion collisions are of great importance in this study; when two large nuclei collide, the nuclear matter is compressed, and due to two-body collisions of the nuclear constituents the temperature rises. Unlike for macroscopic matter, for nuclear matter this state is unfortunately not directly observable: both the length and the time scale of nuclear collisions prohibit probing nuclear matter while it is still at high temperature and density. Instead, the nuclear matter already cooled, expanded, and formed more stable configurations before detection.

However, these late reaction products still carry information that helps to reconstruct what happened in the early stages of the collision. It is the task of simulations to aid the reconstruction of the reaction mechanism and conditions from the late reaction products.

In this thesis, computer simulation tools for nuclear reactions are used to examine the consequences of different microscopic models.

To my wife Anna

Contents

List of Tables

List of Figures

Chapter 1

Introduction

1.1 Intermediate Energy

1.1.1 Percolation Models

In intermediate energy heavy-ion collisions, the production of complex fragments still is a puzzling aspect of nuclear physics research. Experiments have been conducted both with proton and with heavy-ion beams, and several seemingly different phenomena, such as evaporation, spallation, fission and multi-fragmentation have been observed.

In multi-fragmentation scenarios, the hot nuclear system tends to decay into multiple intermediate mass ($3 \leq Z \leq 20$) fragments (IMFs). Significant differences in the relationships between fragment, neutron, and charged particle multiplicities were found between ^{112}Sn+^{112}Sn and ^{124}Sn+^{124}Sn collisions at 40 MeV/A [Kun96]. The results are incompatible with a universal scaling of the average number of intermediate mass fragments versus the number of charged particles and neutrons, respectively, and in Chapter 2, the possibility to explain this phenomenon in the framework of percolation models is explored. It was found that the results are only reproducible in part, which indicates contributions of nuclear phenomena beyond geometrical fragmentation schemes.

1.1.2 Transport Models

For a long time, simulations of heavy-ion collisions have been rather phenomenological in nature, which somewhat corresponded to early experiments being conducted in an inclusive way – phenomenological models, even if based on different assumptions, would predict the inclusive data with oftentimes almost equal quality. As experiments became more sophisticated and exclusive, the need for advanced simulation methods arose. This was when microscopic models became more popular: one has to be able to dynamically simulate the collisions without any assumption concerning thermal equilibrium – transport models are one of those microscopic dynamical models.

Boltzmann-Uehling-Uhlenbeck (BUU) (also called Landau-Vlasov) codes are semi-classical simulations, in which as an ansatz for the Wigner-function a product of Delta-functions is used. Each Delta-function can be associated with a localized "test-particle." Inserting this ansatz into the Boltzmann equation results in equations of motion for the testparticles that are governed by two terms: a smooth modification of the trajectories resulting from a mean-field term, and a collision term that describes two-particle collisions between testparticles. The actual solution of the Boltzmann equation is achieved by evolving the testparticle essemble in phase-space according to the equation of motion rather than solving a partial differential equation. Chapter 3 gives a more detailed overview of this mechanism.

The semiclassical transport codes work reliably at energies beyond 100 MeV per nucleon. Below this energy, quantum effects are too pronounced to be neglected. The BUU codes followed earlier transport codes, so-called cascades,[Cug81] which did not have a mean-field term yet. This approximation is only appropriate at even higher energies, above around 1 GeV per nucleon (Appendix A describes the details of a cascade code). At lower energies, many two-body collisions are blocked due to

phase-space considerations, so that the mean-field term becomes dominant. At higher energies, Pauli-blocking is not so much of an issue anymore, since a large phase-space volume is available, which strengthens the influence of the collision term. At the same time, because the particles have larger momenta, the mean-field becomes less influential.

Transport models have successfully described many aspects of intermediate energy heavy-ion collision dynamics. One of the observables in heavy-ion collisions is the collective flow of the reaction products, it contains information about the compressibility of nuclear matter. However, it was indicated [Ale95] that within current implementations of BUU simulations the equation of state is not implemented in a consistent way. In Chapter 3, a hard core equation of state for the nuclear matter is implemented and its effect on the simulated collective flow is explored.

1.2 Ultrarelativistic Regime

1.2.1 Experimental Efforts

Currently, two colliders are planned for the acceleration of heavy-ions to ultra-relativistic energies. The Relativistic Heavy-ion Collider (RHIC), presently under construction at Brookhaven National Laboratory in New York, is a dedicated heavy-ion collider planned for experiments in 1999. RHIC will accelerate and collide ions from protons to heavy nuclei, such as Au, at c.m. energies up to 500 GeV for protons and 100 GeV per nucleon for Au+Au collisions. The luminosity for Au+Au will be 2 x 10^{26} cm^{-2} s^{-1}. Near head-on collisions of Au+Au at RHIC are expected to produce from 500 to 1500 charged particles per unit pseudorapidity at midrapidity in a single collision.

Large detector systems are being constructed to analyze the products of these interactions to observe indications of the possible formation of a quark-gluon plasma

and a possible chiral phase transition.

Heavy-ion physics research will also be an integral part of the program for the Large Hadron Collider (LHC), to be constructed at CERN, the European Centre for Nuclear Physics, in Geneva, Switzerland. For Pb nuclei, the c.m. energies at the LHC will be 5.4 TeV per nucleon pair with luminosities of 10^{27} cm^{-2}s^{-1}. Predictions for the charged particle densities at the LHC for near head-on collisions of Pb+Pb range from 2000 to 8000 per unit pseudorapidity. The large uncertainty in these numbers arises primarily from the present lack of information on the distributions of soft gluons in nuclei.

1.2.2 Parton-Cascades

It has been indicated that RHIC and LHC run into somewhat of a "theory-vacuum." The interpretation of these complex collisions and the possible generation of a quark-gluon plasma pose a major problem: what are the experimental signatures? Currently, several possible signatures are in discussion:

- Kinematic effects of a first-order phase transition.
- Electromagnetic probes e^+e^-, $\mu^+\mu^-$, γ measure the *early* phase of quark and gluon distributions and content.
- Hadronic probes of deconfinement and chiral symmetry restoration

$$J/\psi \longrightarrow c+\bar{c} \quad (J/\psi,\ \Psi' \text{ suppression})$$

$$gg \longrightarrow s\bar{s} \quad (\text{strangeness enhancement})$$

None of these possible signatures have been commonly acknowledged as reliable. In an effort to aid the answering of this question, a theoretical model for the collision processes that goes beyond a phenomenological description must be developed. One

possible microscopic approach is to extend the semiclassical transport theory to high-energy physics[Kal93, Sor89.1, Sor89.2, Gei92.1, Gei94.1, Gei92.2, Gei93], which leads to so-called "parton cascade" codes. As the energies increase in these models to the ultrarelativistic regime, Lorentz covariance and causality are not strictly respected. The standard argument is that such effects are not important to final results; but they have not been seriously considered at high energies. In Chapter 4, it is pointed out how and why these happen, how serious of a problem they may be and ways of reducing or eliminating the undesirable effects are suggested. The appendix gives a commented listing of the major sections of the parton cascade code that was developed as part of this thesis.

Chapter 2

Isospin dependent multi-fragmentation in ^{112}Sn + ^{112}Sn and ^{124}Sn + ^{124}Sn collisions

2.1 Introduction

Percolation models have proven highly successful in the simulation of multi-fragmentation reactions in the past [Bau84, Cam85]. Within these models, fragmentation is described by first distributing a set of points or sites, each representing a nucleon, on a 3-dimensional lattice, which represents the bonds between the sites. In the case of a simple rectangular lattice, each site is connected to six nearest neighbors, however, it has been shown that the model is to a large degree independent of the lattice structure [Bau84, Sta79]. In the second step, randomly some lattice bonds are broken with a probability that in non-isospin dependent percolation models is the only free parameter. The remaining connected clusters are identified with the fragments of the reaction, the bond-breaking probability with the excitation energy per nucleon [Con79].

In this chapter, the percolation model of Bauer et al. [Bau84] is modified by the explicit inclusion of isospin degrees of freedom, i.e., the lattice is comprised of

protons and neutrons instead of just nucleons, in an attempt to reproduce the experimental data gained in the comparison of the multi-fragmentation in ^{112}Sn+^{112}Sn and ^{124}Sn+^{124}Sn collisions [Kun96]. We especially focus on the average number of intermediate mass fragments (IMFs, $3 \leq Z \leq 20$) $\langle N_{\mathrm{IMF}} \rangle$ versus the number of charged particles N_c (Fig. 2.1, left panels), and versus the number of neutrons N_n (Fig. 2.1, right panels) detected. The full circles denote the results for the ^{124}Sn+^{124}Sn reaction, the circles the results for the ^{112}Sn+^{112}Sn reaction. The striking feature about these distributions is the "splitting" of $\langle N_{\mathrm{IMF}} \rangle (N_c)$, and the position of the maxima in $\langle N_{\mathrm{IMF}} \rangle (N_n)$. Both do not agree with common multi-fragmentation models, in which the distributions $\langle N_{\mathrm{IMF}} \rangle (N_c)$ should lie on top of each other, and the positions of the maxima in $\langle N_{\mathrm{IMF}} \rangle (N_n)$ should simply correspond to the ratio of neutron abundances in the respective isotopes.

Figure 2.1: Average number of intermediate mass fragments (IMFs) versus number of charged particles (left panels) and neutrons (right panels). The full circles denote the experimental results [Kun96] for a ^{124}Sn+^{124}Sn collision, the open circles the results for a ^{112}Sn+^{112}Sn collision, both at 40 MeV/A. The solid lines represent percolation simulation results for the heavier isotopes, the dashed lines for the lighter ones. The top row was calculated without any stability mechanism, in the second row, an evaporation mechanism is employed, in the third row a fission mechanism, the fourth row was achieved with a combination of both.

Figure 2.1

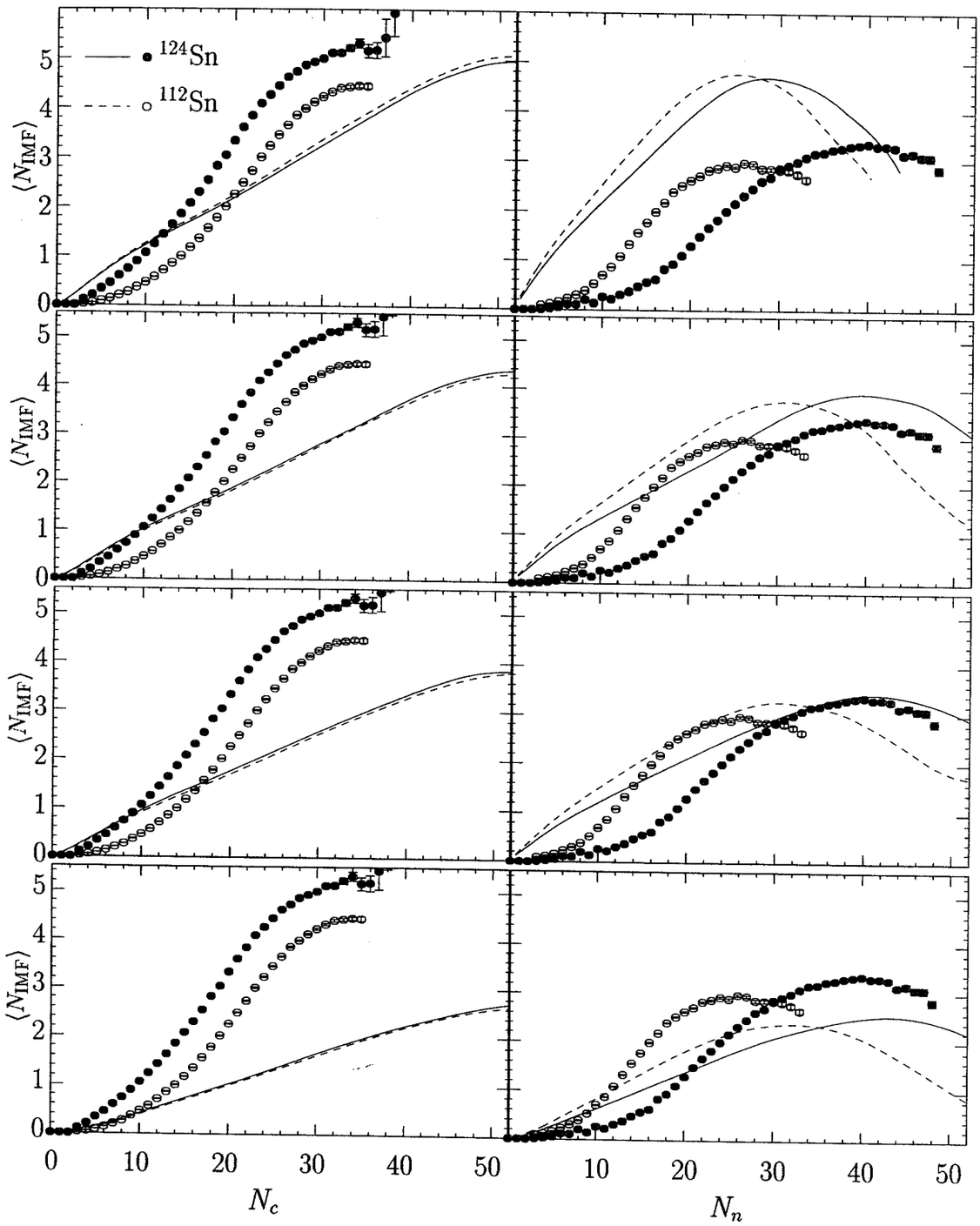

2.2 Implementation of the Isospin Dependent Percolation Model

For each simulated collision event, first the impact parameter is randomly selected. Then with a simple Monte Carlo integration, the number of protons and neutrons in the overlap zone of the two nuclei is determined. We employ an approximation in which the nucleons outside the overlap zone are neglected – we found this approximation to be appropriate by studying Boltzmann-Uehling-Uhlenbeck (BUU) simulations [Bau86] of the collisions at different impact parameters, which clearly showed distinct spectator regions in the final state even for small impact parameters. Figure 2.2 shows the outcome of the BUU simulations at different impact parameters. The simulations were run with $b = 1, 3$, and 5 fm, respectively, and the spectator regions were observed even 200 fm/c later.

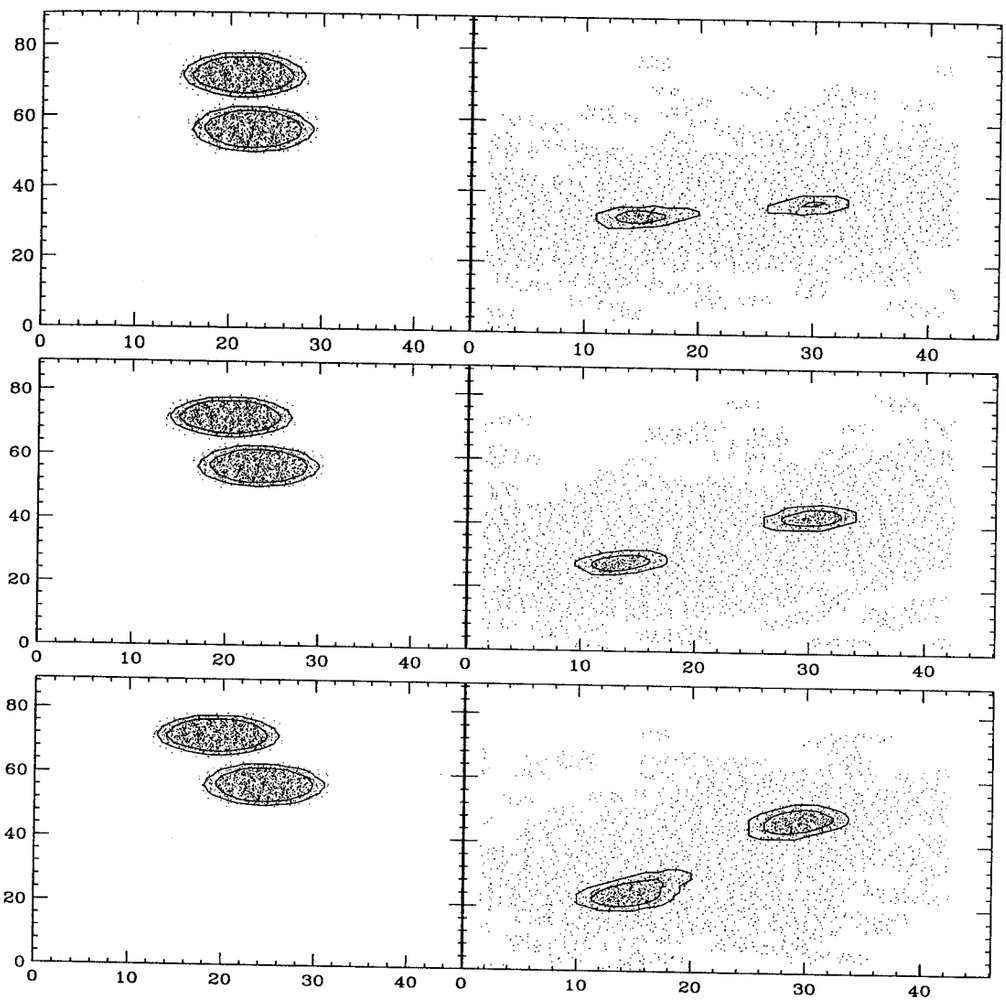

Figure 2.2: BUU simulations of the 40 MeV/A Sn-collisions at different impact parameters. The top plot was done with $b = 1$fm, the middle one with $b = 3$fm, and the bottom one with $b = 5$fm. The left plots show the initial configuration, the right plots the same scenario 200 fm/c later.

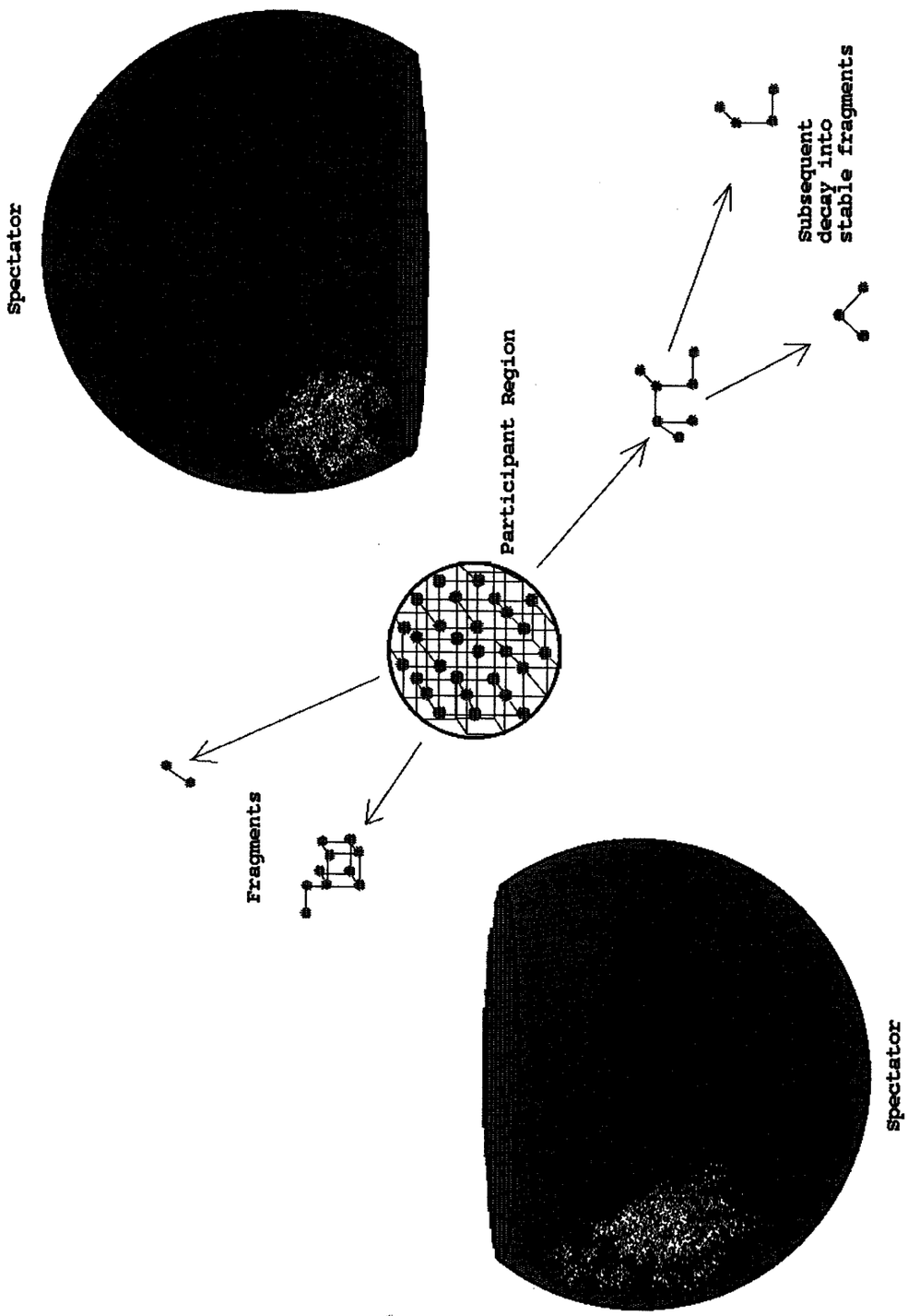

Figure 2.3: The nucleons in the participant (overlap) zone of the nuclei are distributed on a rectangular lattice. Bonds within the participant region are randomly broken, for the resulting fragments, different stability mechanisms are employed.

The nucleons in the overlap zone are randomly distributed on a rectangular lattice (see Figure 2.3).

The lattice bonds are then broken with a probability p, which we determined in two different ways: in one method we set it equal to a parameter p_0 which we obtain by fitting to the experimental data [Kun96], in the second method we choose p according to a Gauss distribution around p_0, i.e., for each simulation, p varies slightly in order to simulate excitation energy fluctuations. A comparison between both methods showed no significant difference in the outcome except for better statistics in the latter method for higher event multiplicities as large bond-breaking probabilities were included. Since we find the inclusion of excitation energy fluctuations to be more realistic, we settled for the latter method.

We then identify clusters of nucleons which are still connected with each other. However, since those clusters are not necessarily a stable configuration of protons and neutrons, we experimented with several different algorithms to achieve fragment stability (see Fig. 2.3). Methods included a re-distribution of protons and neutrons between the fragments, further fission of the fragments, evaporation of protons and neutrons from the fragments, and simulations with no additional stability criteria applied. Also, the definition of stability is not obvious: the experimental lifetime data applies to nuclei in their ground state and is not directly transferable to the fragments of a multi-fragmentation reaction. Since we found the outcome to only be slightly dependent on the definition used, we settled on a stability criterion where the fragments are required to have a ground state lifetime that is long enough for them to reach the detectors. As an unfortunate side effect of fission and evaporation mechanisms, however, the relationship between the bond breaking probability p_0 and the excitation energy is not obvious anymore, rather the combination of the initial bond-breaking and further mechanisms leads to an effective bond-breaking probability

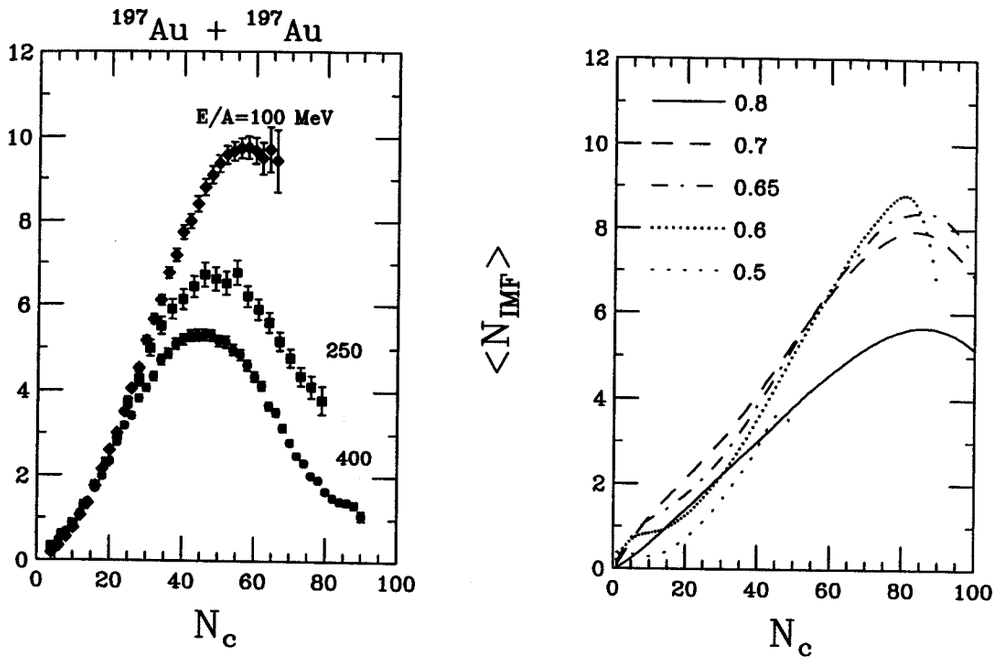

Figure 2.4: Experimental data [Tsa93] and percolation results for a ^{197}Au+^{197}Au collision. The experimental data is given for E/A=100, 250 and 400 MeV, the theoretical predictions refer to different bond-breaking probabilities p_0.

that is higher than p_0 — therefore, p_0 sets a lower limit for the excitation energy.

Of the order of $10^6 - 10^7$ events were simulated for each set-up; for each individual event the number of charged particles, neutrons and IMFs was recorded, where in accordance with the experimental data we employed detector efficiencies of 0.9 for all charged particles and 0.65 for neutrons.

2.3 Results and Conclusions

The code was first applied to the experimental results of Ref. [Tsa93]. Figure 2.4 shows the the average number of intermediate mass fragments ($3 \leq Z \leq 20$) versus the number of charged particles ($\langle N_{\rm IMF}\rangle(N_c)$) for ^{197}Au+^{197}Au collisions. The experimental results in the left panel refer to different energies per nucleon [Tsa93], the curves in the right panel to percolation simulations at different bond-breaking proba-

bilities p_0. It had been found earlier [Pha92] that percolation codes generally slightly underpredict the number of intermediate mass fragments, which was attributed to the possible existence of non-compact decay geometries. Overall, however, the model was found to reproduce the data reasonably well.

In the next step, we address the question of the reproducibility of the isospin-dependence found in Ref. [Kun96]. The top row of Fig. 2.1 shows the result of a simulation with a bond-breaking probability distribution centered around $p = 0.7$ and a half-width of 0.1. In this simulation, no stability mechanism is applied. The solid line corresponds to the simulation for the heavier isotope (experimental data indicated by full circles), the dashed line to the lighter isotope (open circles). The difference between the isotopes in the average number of IMFs versus the number of charged particles could not be reproduced, the outcome basically reflects the trivial autocorrelation that every IMF is a charged particle, the slope is determined by the ratio of IMFs versus lighter fragments. The linear relationship will eventually break down in events with high multiplicities when more and more fragments are smaller than IMFs. The experimental data shows that in the heavy isotope relatively fewer fragments with $Z < 3$ are formed, a trend that cannot be seen in the simulation. The difference in the average number of IMFs versus number of neutrons (right panel) can be reproduced, which, however, is not surprising: in the collision of the neutron-richer isotopes, more neutrons are emitted. The positions of the maxima, i.e., at 25 and 29 neutrons, respectively, correspond to the ratio of neutrons in the isotopes, 62 and 74, respectively ($25/29 \approx 0.86; 62/74 \approx 0.84$). In the experimental data the maxima are at 25 and 40 neutrons, the ratio of ≈ 0.63 is in-compatible with the simple explanation above. At high neutron numbers, statistics get rather unsatisfactory, and we do not reproduce the high neutron multiplicities seen in the experiment for the heavy isotope.

The second row of Fig. 2.1 shows the outcome of a simulation with an evaporation mechanism to achieve fragment stability: protons and neutrons are broken off the fragments until the remainder is stable. In the simulation shown, in case of $N > Z$, neutrons are broken off, and vice versa. In another simulation, protons and neutrons had been broken off randomly, which lead to slightly less IMFs. Again, differences in the IMF-distribution versus number of charged particles (left panel) could not be observed, however, for both isotopes, in comparison to the simulation without stability criterion,the ratio of IMFs to lighter particles decreased. In the IMF distribution versus number of neutrons (right panel), naturally higher neutron multiplicities are observed, the ratio of the maxima positions (32/40=0.8) remains compatible with the ratio of neutrons between the isotopes, though.

The third row of Fig. 2.1 results from a simulation a fission mechanism: an unstable fragment is broken into two fragments, if such a secondary fragment is unstable, it is again broken up into two fragments, and so on, until only stable fragments remain. The distribution of the secondary fragment sizes is chosen to be centered around 0.5 and falls off quadratically towards 0 at 0 and 1; a simulation with a flat distribution yielded similar results, it had only very slightly less IMFs. Both these mechanisms fit the IMF distribution versus number of neutrons rather well, the ratio of the positions of the maxima, $31/41 \approx 0.7$ is half-way between the expected 0.83 and the experimental 0.6, however, the different heights of the maxima could not be reproduced. The IMF-distribution versus charged particles again fails to show differences between the isotopes.

The forth row finally shows the result for a combination of the two mechanisms above, each unstable fragment undergoes evaporation or fission with equal probability. Apparently, this mechanism produces too many light fragments, both charged particles and neutrons. The ratio of the maxima in the IMF distribution versus number

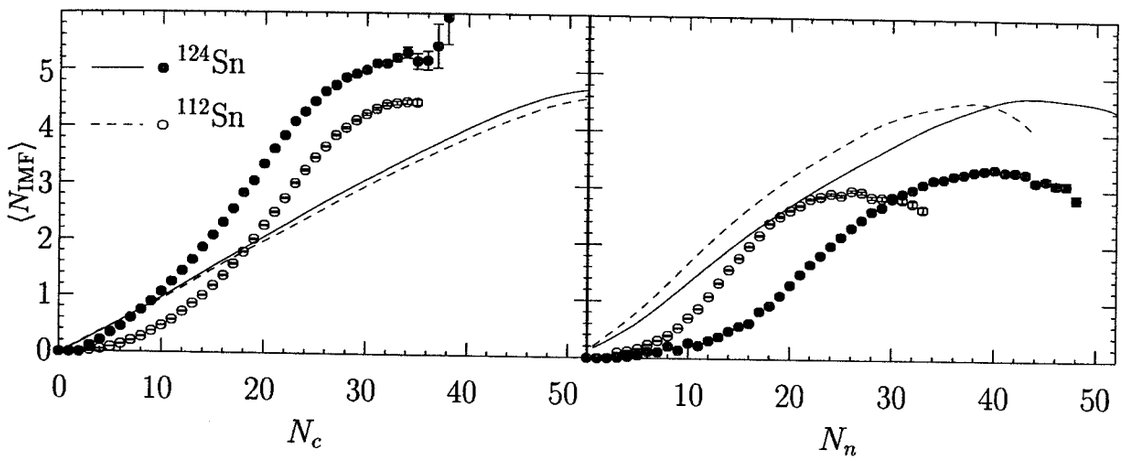

Figure 2.5: Results of a simulation with different bond-breaking probabilities for equal and different nucleon bindings ($p_{0d} = 0.6$; $p_{0e} = 0.9$).

of neutrons is 33/44=0.75.

In deviation from the established percolation models, we also worked with different break-up probabilities for bonds between protons and protons, neutrons and neutrons, and protons and neutrons, that is, a probability p_{0e} for equal pairings, and a probability p_{0d} for unequal pairings, $p_{0e} \geq p_{0d}$. As it turns out, in this method the outcome depends significantly on the distribution of protons and neutrons on the lattice: in the case of a highly ordered configuration where except for the excess neutrons both types of nucleons are distributed in an alternating way ("salt crystal"), i.e., in general every proton has six neutrons as nearest neighbors and vice versa, the excess neutrons being put in randomly as "impurities," one notes significant differences between both Sn-isotopes in the distribution of intermediate mass fragments versus charged particles – however, these are still much smaller than in the experiment, as Fig. 2.5 illustrates this for $p_{0e} = 0.9$ and $p_{0d} = 0.6$. Even though this effect leads to a slightly closer resemblance of the experimental data, we consider it to be an artifact since it nearly completely vanishes with a purely random distribution of protons and neutrons on the grid. We attribute this effect to the fact that in a pure "salt-crystal"

configuration every bond has the break-up probability p_{0d}; every impurity will in general lead to the introduction of six bonds with break-up probability p_{0e}, and therefore has a large impact. As a result, disregarding surface effects, in the collision between the lighter isotopes about 79% of the bonds are of type p_{0d} and 21% of type p_{0e}, while for the heavier isotopes the percentages are 61 and 39, respectively. In the random configuration, however, there is no such amplification, the percentages are 58 versus 42 for the lighter isotope, and 56 versus 44 for the heavier isotope.

Also, simulations were run with a "neutron skin," which influenced the ratio of protons and neutrons in the overlap zone for different impact parameters: for small impact parameters the ratio of neutrons to protons was higher than for large impact parameters, the size of the neutrons skin were determined by a Hartree-Fock calculation[Bro96]. However, also these simulations could not improve the agreement with experimental data.

In conclusion, the experimental results could only be reproduced in part. The main discrepancies are:

- The difference between the two isotopes in the average number of IMFs versus number of charged particles could not be reproduced.
- The difference in the maximum values of the IMF distributions versus number of neutrons could not be reproduced.
- The experimental positions of the maximum number of IMFs versus number of neutrons is in-compatible with the trivial shifting due to higher neutron abundance that is found in the simulation.

The discrepancies found between the data and this basically geometrical approach indicate that effects outside of percolation theory are important. The nuclear struc-

ture of the fragments as well as sequential feeding might play a role. Most important however seems the role of preequilibrium emission which may not only effect the sorting axis but as well determines the N/Z composition of the fragmenting system.

Chapter 3

Nuclear Flow in Consistent Boltzmann Algorithm Models

3.1 Introduction

Heavy-ion collisions are of great importance in answering the question how nuclear matter changes its properties under different temperatures and pressures.[Cze86] When two large nuclei collide, the nuclear matter is compressed, and due to two-body collisions between nuclear constituents also the temperature rises to about 50 – 100 MeV (about 5 to 10 times 10^{11} Kelvin). Unlike for macroscopic matter, for nuclear matter possible phase transitions etc. are unfortunately not directly observable: both the length (about 10 fm=10^{-14} m) and the time scale (about 60 fm/c =2×10^{-22} seconds) of nuclear collisions prohibit probing the nuclear matter while it is still at that high temperature and density. Instead, the nuclear matter has already cooled down, expanded, and formed more stable configurations before it hits the detectors; every observation can only be indirect.

However, these late reaction products still carry information that helps to reconstruct what happened in the early stages of the collision. For example, the collective flow of the reaction products contains information about the compressibility of nuclear matter. With the exception of the merely theoretical case of a head-on collision

of the two nuclei (vanishing impact parameter), from straightforward considerations it is expected that in the collision nuclear matter of the two partners is pushed outwards perpendicular to the beam within the plane defined by the impact parameter. The harder in the sense of compressibility the nuclear matter would be, the stronger this effect would be expected to be. Also, from this very simple consideration one would expect the flow to always increase with the beam energy. However, since the interaction between nucleons in addition to a short range repulsion has a long range attraction, this simple picture does not hold true: at low energies, the long range part of the nuclear interaction dominates, the nucleons are attracted, and flow is generated by the nucleons being scattered *towards* each other. At energies around 70-140 MeV/nucleon depending on the mass of the reaction partners both effects cancel out each other, the flow disappears in the experiment; simulations to-date tend to underpredict that value.[Wes86] At high energies, the nucleons collide at short range, and the mechanism for flow indeed corresponds to the simple consideration above.

To extract quantitative information about and gain insight into the microscopic processes within nuclear matter, however, it is necessary to have a dynamical model to simulate the collisions themselves. Comparision between the predictions for the final stage gained by the simulation on the one hand, and the actual experimental results on the other hand are used to refine the model for the early stages. The simulation of heavy-ion collisions unfortunately is equivalent to solving a quantum-mechanical many-body problem, which to date is not fully possible. Different approaches have been made to nevertheless approximate the solution. Early approaches were based on hydrodynamics, they used a nuclear equation of state, but the mean free path of the nucleons was assumed to be so small that the nuclei in the collision merely resembled splashing droplets. At the other extreme, there were models that due to their extremely long mean free path basically resembled colliding gas clouds.[Das93]

To model the situation more realistically, testparticle based models were developed. Here, a nucleon and other nuclear constituents are represented by a number of testparticles, their individual trajectory is followed rather than being concerned only with the global properties of some nuclear "fluid" or "gas." Obviously, these microscopic methods, which can be implemented in different ways, have the general property of being computationally more intense than the macroscopic ones.

One method is that of Molecular Dynamics,[Aic91] in this method both the long-range attractive (soft) and the short-range repulsive (hard) part of the particle interaction is parametrized by potentials, the trajectories of the testparticles are continously updated in response to the local potential.

Another semi-classical particle-based method is the Boltzmann-Uehling-Uhlenbeck (BUU) approach. Here the soft part of the interaction is represented by mean fields, while the hard part is given by an explicit collision term. The collision term itself can again be represented in different ways, especially the criteria for a collision to happen are model dependent. In many codes, this decision is based on geometrical considerations, for example, a collision is generated at the point of closest approach between two particles. The BUU method is being used by various groups.[Ber88, Aic96, Bau86]

One particular implementation of the collision term in BUU codes is the Direct Simulation Monte Carlo approach (DSMC), see for example Lang et al.,[Lan93] and Danielewicz.[Dan95] In this approach, collisions between the testparticles are not generated through geometrical and particle-trajectory based criteria, but stochastically in a way that the correct collision rate is reproduced. In a collision only momenta and energy of the particles are changed, while the particles themselves stay in place until the next advection step – the particles are assumed to be pointlike.

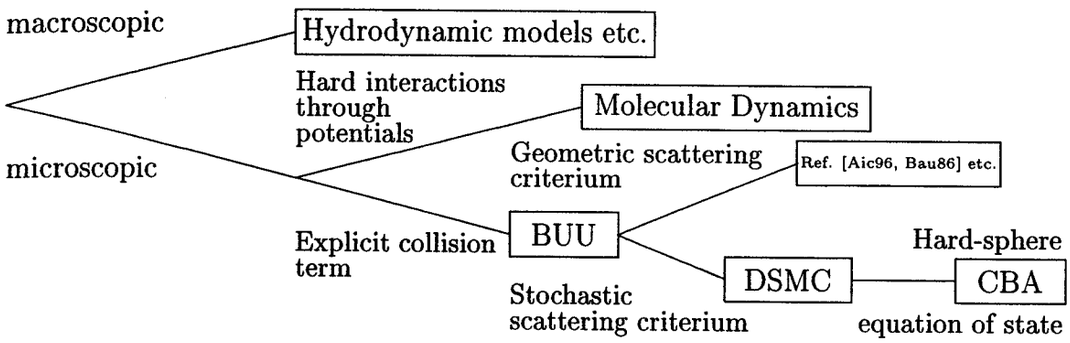

Figure 3.1: Overview of techniques to simulate heavy-ion collisions.

It was suggested that in order to reproduce a Hard-Sphere Boltzmann Equation, the DSMC approach should be extended by an additional advection that should take place after any collision,[Ale95] and by a modification the collision probability itself[Ale95, Res77] (Enskog Theory).

Figure 3.1 summarizes these different techniques.

This advection is supposed to push the collision partners away from each other according to their hard-sphere radius, and the collision probability is adjusted to take into account the excluded volume of the hard spheres and screening and shadowing effects. The modified DSMC method is called Consistent Boltzmann Algorithm (CBA). The modifications ensure a non-vanishing second virial and change the equation of state for the scattering process from that of an ideal gas to that of a hard-sphere gas; their effect on the calculated value of directed nuclear collective flow in heavy ion collisions is analysed, and it is found that the flow slightly increases.

3.2 Theoretical Background

In the DSMC approach, the positions and momenta of the particles are evolved in a two-step process, namely advection and collisions, corresponding to one timestep of the simulation. During the advection step the particles are propagated according to their momenta. During the collision step first the particles are sorted into spatial cells of volume V. Then out of the n particles within a given box, at random, m combinations are chosen and scattered with the probability

$$W = \frac{\sigma(\sqrt{s}) v_{\rm rel} \Delta t}{NV} \frac{n(n-1)/2}{m} \ , \tag{3.1}$$

where $\sigma(\sqrt{s})$ is the energy-dependent elementary hadron-hadron cross section, N is the number of testparticles representing one nucleon in a full-ensemble testparticle algorithm [Wel89], Δt is the timestep length, and $v_{\rm rel}$ is the relative velocity of the particle pair [Lan93]. In the limit $V \to 0$, $\Delta t \to 0$, $N \to \infty$, the solutions of this method have been shown to converge to the exact solution of the Boltzmann equation (without mean field contribution)[Bad89],

$$\partial_t f_1 + \boldsymbol{v} \cdot \frac{\partial f_1}{\partial r} = (\partial_t f_1)_{\rm coll} \ . \tag{3.2}$$

Here, $f_1(\boldsymbol{r}, \boldsymbol{v}; t)$ is the *one particle distribution function* , which, according to Boltzmann, is defined in such a way that

$$f_1(\boldsymbol{r}, \boldsymbol{v}; t) \ d\boldsymbol{r} \ d\boldsymbol{v}$$

is the number of particles that at a time t are within a volume element $d\boldsymbol{r}$ around $\boldsymbol{r}$ and have a velocity $d\boldsymbol{v}$ around $\boldsymbol{v}$. The infinitisimal volume elements have to be taken with a grain of salt, since taken literally, within a *mathematically* infinitisimal volume element, f_1 could either be '1' or '0' – the pointlike particle could either be inside the infinitisimal volume, or not. Rather, the volume element has to be a *physical* element